catalysts

MDPI

Article

$DeNO_x$ Abatement Modelling over Sonically Prepared Copper USY and ZSM5 Structured Catalysts

Przemysław J. Jodłowski [1,*], Łukasz Kuterasiński [2], Roman J. Jędrzejczyk [3], Damian Chlebda [4], Anna Gancarczyk [5], Sylwia Basąg [4] and Lucjan Chmielarz [4]

1 Faculty of Chemical Engineering and Technology, Cracow University of Technology, Warszawska 24, 31-155 Kraków, Poland
2 Jerzy Haber Institute of Catalysis and Surface Chemistry, Polish Academy of Sciences, Niezapominajek 8, 30-239 Kraków, Poland; nckutera@cyf-kr.edu.pl
3 Malopolska Centre of Biotechnology, Jagiellonian University, Gronostajowa 7A, 30-387 Kraków, Poland; roman.jedrzejczyk@uj.edu.pl
4 Faculty of Chemistry, Jagiellonian University, Ingardena 3, 30-060 Kraków, Poland; damian.chlebda@uj.edu.pl (D.C.); basag@chemia.uj.edu.pl (S.B.); chmielar@chemia.uj.edu.pl (L.C.)
5 Institute of Chemical Engineering, Polish Academy of Sciences, Bałtycka 5, 44-100 Gliwice, Poland; anna.g@iich.gliwice.pl
* Correspondence: jodlowski@chemia.pk.edu.pl; Tel.: +48-12-628-27-60

Academic Editors: Luis M. Gandía, Mario Montes and José Antonio Odriozola
Received: 24 May 2017; Accepted: 30 June 2017; Published: 6 July 2017

Abstract: Metallic supports play an important role as structured reactor internals. Due to their specific properties including enhanced heat and mass transport, high mechanical resistivity and elimination of local hot-spots, they are commonly used in gas exhaust abatement from stationary and automotive industries. In this study, the performance of three structured supports with deposited Cu/USY (Ultrastabilised Y—zeolite) for $deNO_x$ abatement were modelled. Based on kinetic and flow resistance experimental results, the one-dimensional (1D) model of structured reactor was developed. The performance of the structured reactors was compared by the length of the reactor necessary to achieve an arbitrary 90% NO_x conversion. The performed simulations showed that the sonochemically prepared copper USY and ZSM-5 zeolites deposited on metallic supports may be successfully used as catalysts for $deNO_x$ process.

Keywords: structured reactors; $deNO_x$ selective catalytic reduction (SCR); zeolites; modelling

1. Introduction

The problem of NO_x removal from stationary and automotive sources seems to be one of the most important issues in gas exhaust abatement. The NO_x is produced mainly in the processes where the fuel is combusted in a combustor at high temperatures with the high amount of N_2. The mechanisms of NO_x formation are known and they have been widely discussed in literature [1–5]. Over the various NO_x sources, the stationary and mobile ones have the most significant impact on environmental pollution. Due to this fact, in most countries the limits on the NO_x emissions have been established for power plants, gas turbines and vehicles. Particular attention must be paid to the biogas powerplants, where the NO_x emission strongly depends on the type of biomass used during the fermentation process [6].

Over the years, many great efforts have been paid to develop efficient technology for $deNO_x$ removal. The developed selective catalytic reduction technology, using NH_3 as a reducing agent, seems to be the most effective one, due to high conversion and selectivity of NO_x to nitrogen and water [7]. Through the years, many catalytic systems have been developed, including the commercially used vanadia-supported titania catalyst promoted with WO_3 or MoO_3 and zeolite based catalysts. The

latter obtained much attention due to the possibility of their being used at temperatures up to 600 °C, at which the use of transitional metal oxide catalysts is limited due to their thermal liability [7].

The preparation of the active catalysts for deNO$_x$ purposes proceeds via conventional ion exchange, by introducing the transitional metals into the zeolite structure to compensate the negative charge of zeolite framework [8]. Recently, the literature has provided examples of use of ultrasonic irradiation for the preparation of zeolites [9,10]. The use of the sonochemical approach for the zeolite synthesis reduces the time and temperature during the preparation, and may increase the crystallinity of the prepared zeolites [11]. However, the information about the use of the sonochemical method for incorporation of metals into the zeolite structure to compensate the zeolite framework negative charge is not discussed widely.

On the other hand, the development of alternative catalytic systems for the industrial applications cannot be considered without its deposition onto the structured supports, which are commonly used for the commercial deNO$_x$ abatement purposes [7]. In the literature reports, the short channel structures as well as metallic foams have recently been reported as having a great potential as catalyst supports for gas exhaust abatement [12–16]. In our previous works [12,17,18], we reported the superior activity of ion-exchanged Cu/SSZ-13 and Cu/ZSM-5 zeolite catalysts deposited on kanthal plates and foams. In the literature, the deposition of the zeolites onto the metallic supports is performed via dip-coating of the support in the zeolite suspension or zeolite gel [7]. However, our recent development on zeolite deposition revealed that the deposition of the zeolites using dip-coating from zeolite suspension does not provide the efficient support coverage and, what is more important, does not have the efficient mechanical resistance [18]. In recent study [18], we reported the comparison of the deposition of the MFI zeolite onto the metallic supports using dip-coating, in situ deposition and in situ deposition on non-calcined support. The mechanical strength of the deposited zeolite was measured by the application of ultrasound test, where the supports with the deposited zeolite material were placed in an ultrasound bath and irradiated with 35 kHz for 1 h in acetone solution. For the dip-coated catalysts, the measured weight loss exhibited that the overall material was detached from the support, while for in situ deposition and in situ deposition on non-calcined samples, the weight loss did not exceed 30%.

However, to entirely describe the performance of the zeolite catalysts at industrial conditions, the modelling of the structured reactor should be performed.

In this study, the performance of the reactors composed of short channel gauzes or a metal foam structure in deNO$_x$ selective catalytic reduction (SCR) reaction were modeled and compared with the classical ceramic monolith. The catalysts were prepared by sonochemical preparation and as a reference by ion-exchange method. The kinetics as well as mass transport characteristics for modelled structures were determined experimentally.

2. Results

2.1. Kinetic Results

The results of the catalytic activity measurements are presented in Figure 1.

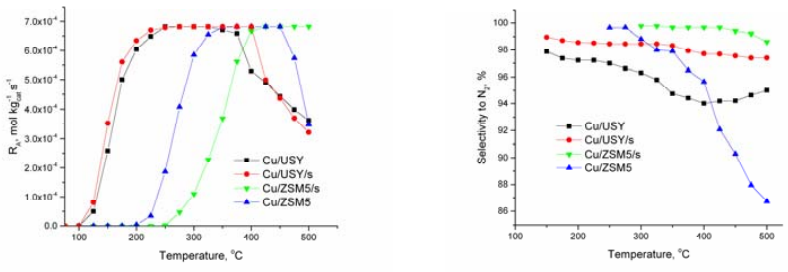

(**a**) (**b**)

Figure 1. *Cont.*

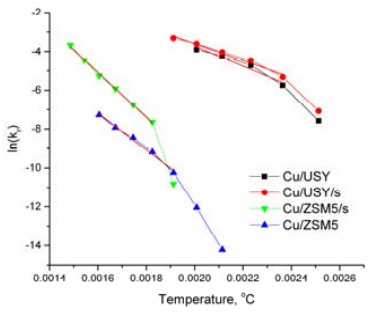

(**c**)

Figure 1. Kinetic results of selective catalytic reduction (SCR) deNO_x over various zeolite catalysts: (**a**) reaction rate; (**b**) N_2 selectivity in SCR of NO with NH_3; (**c**) Arrhenius plot based on kinetic results presented in (**a**).

It can be seen that all prepared catalyst samples revealed complete NO conversion (Figure 1a). The best activity was obtained by Cu/USY/s—catalysts prepared by sonochemical preparation route. The complete conversion was achieved at 225 °C. The comparable activity was obtained by its counterpart prepared by conventional ion-exchange. However, it is worth mentioning that the comparison of the copper content, determined by atomic absorption spectroscopy (AAS) (Table 1), in sonochemically prepared sample (Cu/USY/s) is ca. 25% lower than in Cu/USY sample.

Table 1. Catalysts preparation and characterization details.

Catalyst	Preparation Method	Si/Al	Copper Content *, wt %	Preexponential Factor, k_∞, $m^3/kg\ s$	Activation Energy, E_a, kJ/mol	η **
Cu/USY	Ion-exchange	4.52	4.90 ± 0.05	1.18×10^1	42.76	-
Cu/USY/s	Sonication	4.52	3.70 ± 0.04	1.66×10^2	36.21	1
Cu/ZSM5	Ion-exchange	37	0.320 ± 0.003	2.72×10^3	78.39	-
Cu/ZSM5/s	Sonication	37	0.130 ± 0.001	1.10×10^4	96.01	1

* determined by atomic absorption spectroscopy (AAS); ** calculated Thiele modulus equals 0.05 assuming 20 μm catalyst layer.

When comparing the activity of ZSM-5 catalysts, the best was obtained by sample prepared by conventional ion-exchange method, Cu/ZSM-5. The complete NO conversion was achieved at 350 °C, whereas for catalysts prepared by sonochemical method, the maximum NO conversion was shifted to 400 °C. However, to comprehensively compare the overall performance of copper exchange zeolite catalysts prepared by both conventional and sonochemical methods, the selectivity towards N_2 should also be considered. The selectivity curves are presented in Figure 1b. It must be emphasized that for all catalysts prepared by sonochemical route, the selectivity is almost constant, and for Cu/ZSM-5/s sample, varies between 99% and 100%, whereas for the most active catalyst sample, Cu/USY/s, the selectivity varies from 99% at 150 °C to 98% at 500 °C. For Cu/USY catalyst sample, the most significant decrease in selectivity can be noticed at 400 °C, reaching the selectivity to N_2 equals 94%. The lowest and the most visible decrease in selectivity was observed for Cu/ZSM-5 sample, for which the selectivity drops from 100% at 250 °C to 86% at 500 °C. When considering the deNO_x reaction selectivity, the impact of N_2O that could be formed during the reaction cannot be neglected. Since the N_2O have a strong greenhouse gas, it may affect the whole SCR process. In this study, the series of the Cu/USY and Cu/ZSM-5 catalysts varying the method of preparation are described. As presented in the catalytic activity tests (Figure 1a), the high catalytic activity windows are different for both catalysts. The Cu/USY and Cu/USY/s catalysts are active in low temperature region (starting from 200 °C), which is below the temperature region for commercially used V_2O_5-TiO_2. At low temperature

regions, the selectivity to N_2O is low and does not exceed 6%. On the other hand, when considering the high temperature $deNO_x$ catalysts (Cu/ZSM-5/s, Figure 1b), the selectivity to N_2O was below 1%.

To compare the catalysts performance, the Arrhenius equation parameters were determined according to the Arrhenius equation (Equation (9)). The Arrhenius plots are presented in Figure 1c. It can be inferred that the lowest activation energies were obtained for faujasite catalysts, where apparent activation energy was equal to 42.76 and 36.21 kJ/mol for Cu/USY and Cu/USY/s catalysts, respectively. The higher activation energies were obtained for Cu/ZSM-5 and Cu/ZSM-5/s and equal to 78.39 and 96.01 kJ/mol, respectively. The calculated values are typical for copper exchange zeolite catalysts for $deNO_x$ abatement and are close to those found in the literature for similar catalytic systems [19–21].

Based on the catalytic activity tests of the prepared zeolite catalysts, for modelling purposes, the modelling of structured reactors in SCR $deNO_x$ was performed for catalysts prepared by sonochemical route, Cu/USY/s and Cu/ZSM-5/s, respectively.

2.2. Modelling Results

The modelling results for both Cu/USY/s and Cu/ZSM-5/s catalysts are presented in Figure 2.

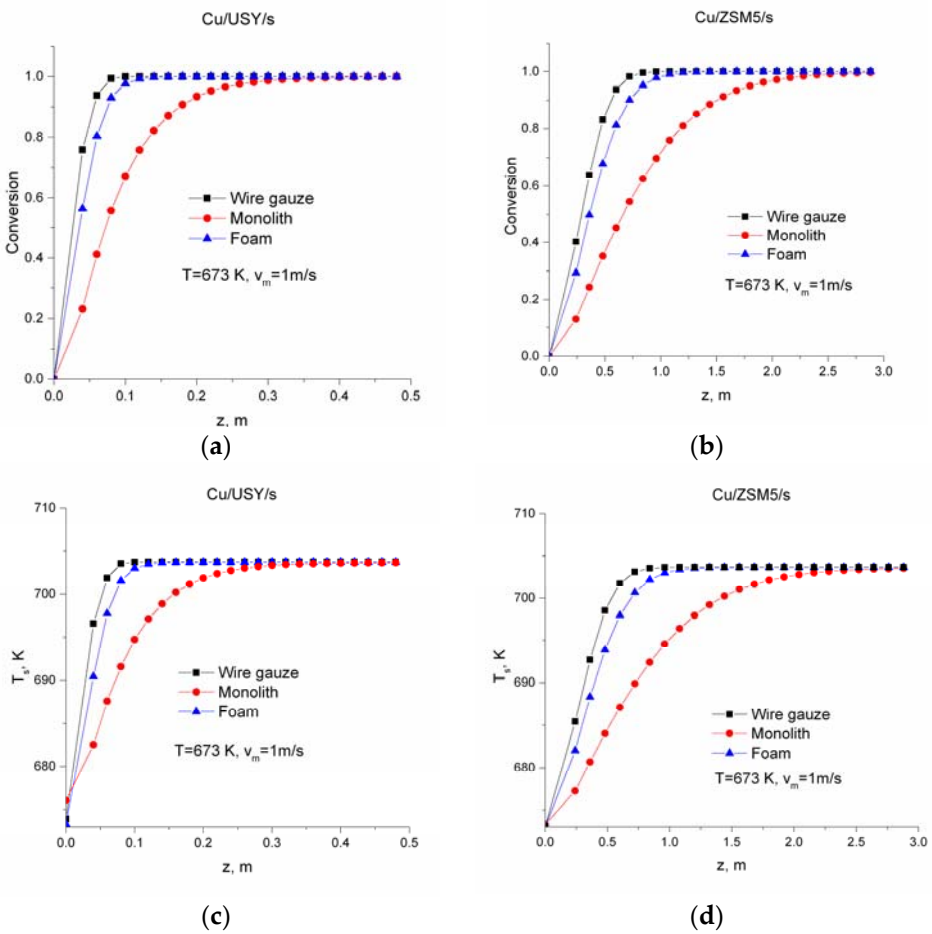

Figure 2. Comparison of different structured supports; superficial gas velocity 1 m/s, inlet gas temperature 673 K, NO concentration: 2500 ppm: (**a**) conversion profile along the reactor for Cu/USY/s; (**b**) conversion profile along the reactor for Cu/ZSM-5/s; (**c**) temperature profile along the reactor for Cu/USY/s; (**d**) temperature profile along the reactor for Cu/ZSM-5/s.

The reactor performance is presented in a form of conversion profiles along the reactor in Figure 2a,b for both Cu/USY/s and Cu/ZSM-5/s, respectively. The reactor performance was also

presented as a temperature distribution along the reactor (Figure 2c,d). Due to the sufficient heat exchange between the surface and the bulk phase, the differences between their temperatures can be neglected. The maximum difference between those two areas does not exceed 3 K at the reactor entrance for the monolith structure. For the wire gauze and foam structured supports, the difference in bulk and surface temperature was as low as 0.3 K at the reactor entrance. Thus, for comparison reasons, the temperature along the reactor was presented only for the bulk phase.

As can be noticed, the performance of the Cu/USY/s catalysts during the NO_x SCR reaction is substantial. It is due to the high activity of the Cu/USY/s obtained during the activity tests. The most significant impact on the modelling results can be attributed to calculated activation energy (Figure 1c). The calculated E_a values for Cu/USY/s and Cu/ZSM-5/s substantially differ and they equal 36.21 and 96.01 kJ/mol, respectively (Table 1). Moreover, the differences between the modelled reactor supports represented by wire gauzes and metal foam are not substantial. The best performance was achieved by the reactor composed of wire gauze structures with deposited Cu/USY/s catalyst (Figure 2a). The nearly complete conversion was achieved after 0.1 m of the reactor. The reactor composed by the foam structure at similar reactor conditions achieves 97% conversion of NO_x's. The small differences between performance of the modelled structured supports are due to the differences between the hydraulic diameters of both wire gauze and foam structures. Despite the slightly slower NO conversion for foam structure, the comparison of the shape of the light-off curve, the most significant differences can be noticed at the very beginning of the reactor. However, the maximum difference in NO_x conversion was noticed at 0.05 m of the reactor. The NO conversion at 0.05 m of the reactor with wire gauze support was equal to 76%, whereas for foam-supported reactor the conversion was 56%. The differences in NO conversion between both foam and wire gauze structures disappear at complete NO_x conversion. On the contrary, the most significant differences at the reactor performance can be observed for modelled 100 cpsi (channels (cells) per square inch) ceramic monolith. The complete conversion achieved by Cu/USY/s catalysts deposited on monolith structure was at 0.46 m reactor. Similar trends can be observed when comparing the surface temperature (Figure 2c). The maximum temperature, ca. 704 K, is achieved and all NO are reduced during the reaction.

On the contrary, the simulation performed for the Cu/ZSM-5/s catalysts reveals that the reactor length required for complete NO conversion in case of reactor composed of wire gauzes is equal to 0.96 m, whereas for reactor composed of foam structure, the required length is equal to 1.44 m. The worst performance was presented by reactor composed of 100 cpsi ceramic monolith. The complete conversion of 2500 ppm of NO is achieved at 2.88 m.

For the assessment of the performance of the reactors composed of all structured supports, the evaluation criteria including reactor length ($L_{R,\ 90\%}$), pressure drop ($\Delta P_{90\%}$) and catalyst mass present on the geometric surface area of the carrier ($M_{cat,\ 90\%}$) were compared and presented in Figure 3.

Over the three modelled structured supports, the wire gauze and foam metallic carriers allow for the substantial shortening of the reactor. The required length of the reactor to achieve 90% conversion of 2500 ppm of NO at 673 K at 1 m/s is equal to 0.06 and 0.08 m for wire gauze and foam carriers, respectively. At the same time, the required length of the reactor with ceramic monolith is almost three times higher and equals 0.18 m. Catalysts loading in both monolith and wire gauze structures, represented by $M_{cat,\ 90\%}$ do not differ substantially. The required amounts of catalysts are equal to 3.86 and 3.84 kg/m^2, for monolith and wire gauze, respectively. Nevertheless, the $M_{cat,\ 90\%}$ calculated for foam structure is slightly higher and equals 4.63 kg/m. The most significant impact on that parameter can be attributed to the specific surface area (a, m^{-1}). Despite the fact that the required lengths of the modelled reactors are three times shorter than in the case of the monolith structure, their specific surface area is more than two times higher (cf. Table 2). When comparing another important engineering characteristic—flow resistance represented by ΔP—the unarguable lowest value was achieved by monolith structure (0.21 kPa). Over the metallic supports, the lowest pressure drop was achieved by foam structure and was equal to 1.34 kPa (Figure 3a).

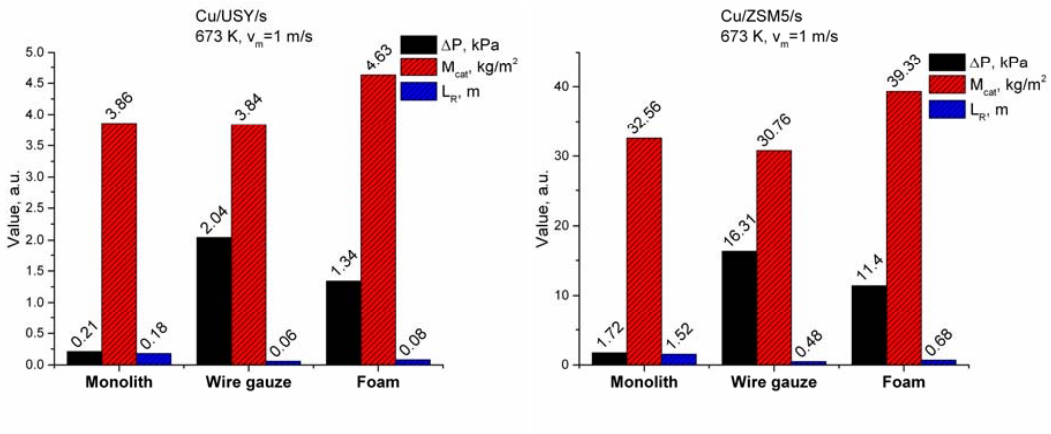

Figure 3. Comparison of reactor supports for an arbitrary assumed final conversion of X = 0.9: pressure drop in reactor (ΔP), reactor length (L_R), catalyst mass per square meter of reactor cross-section (M_{cat}); superficial gas velocity 1 m/s, inlet gas temperature 673 K, NO concentration: 2500 ppm; (**a**) Cu/USY/s; (**b**) Cu/ZSM-5/s.

The comparison of three reactor performance parameters for Cu/ZSM-5/s catalysts reveals similar trends. All calculated reactor characteristics are almost one order of magnitude higher than those obtained for Cu/USY/s catalyst.

Over presented simulations, it is also worth considering the reactor performance at different inlet superficial gas velocities. The results of simulations are summarized in Table 2.

Table 2. Reactor performance for an arbitrary assumed final conversion of X = 0.9 of 2500 ppm NO at 673 K and gas velocities Cu/USY/s catalyst.

Superficial Gas Velocity, m/s	Temperature Reactor Support	673 K L_R, m	673 K M_{cat} *, kg/m^2	673 K ΔP, kPa
v_m = 0.5	Wire gauze	0.028	1.79	0.41
	Metallic foam	0.036	2.08	0.26
	Monolith	0.08	1.71	0.05
v_m = 1	Wire gauze	0.06	3.84	2.04
	Metallic foam	0.08	4.63	1.34
	Monolith	0.18	3.86	0.21
v_m = 2	Wire gauze	0.12	7.69	10.43
	Metallic foam	0.16	7.71	6.70
	Monolith	0.36	9.25	0.87

* catalyst mass, kg/m^2 of reactor cross-section.

The differences between the calculated reactor lengths required to achieve 90% NO conversion at different gas velocities are substantial. It can be inferred that decreasing the gas velocity to 0.5 m/s results in decrease of all parameters. The reactor length and catalyst loading are almost two times lower than at 1 m/s gas velocity. Furthermore, the decrease of gas velocity result in four times the decrease of the pressure drop.

The reversed tendency can be observed for higher velocities. Increasing the superficial gas velocity to 2 m/s results in an increase of the required reactor length to 0.12 and 0.16 m for wire gauze and metallic foam structure, whereas for the monolith structure the reactor length increases to 0.36 m.

3. Discussion

The activity of Cu-modified USY and ZSM-5 zeolites during the deNO$_x$ SCR process over the three different structured supports was considered. In this study, the extraordinary activity of catalysts

prepared using sonochemical preparation route was proposed. In the literature, the activity of USY and ZSM-5 catalyst was previously discussed [18,19,22,23]. However, over the cited literature reference, the copper/zeolite catalysts were prepared by classical ion-exchange method. Despite the fact that the catalysts prepared by classical ion-exchange method also reveal high activity towards the NO_x reduction, their selectivity to N_2 drastically drops at elevated temperature (Figure 1b). Sonically prepared catalysts revealed almost constant 100% selectivity even at temperatures as high as 500 °C. The extraordinary activity and selectivity of sonically zeolite catalysts were not previously reported in literature and require additional deep investigation.

The performance of the sonically prepared Cu/ZSM-5/s and Cu/USY/s catalysts was modelled over three different structured supports: ceramic monolith, metallic foam and stacked wire gauzes. Recently, the application of the metallic supports to gas exhaust abatement has been intensively studied [24–26]. Due to the intense heat and mass transfer parameters, the metallic foams and wire gauze-supported catalysts seem to be the obvious candidates to replace the monolithic reactors. The simulation performed in this study has revealed great activity of metallic supports. The calculated reactor performance characteristics for an arbitrary 90% conversion confirmed that the reactor length can be substantially decreased by the application of either wire gauzes or metallic foams. Additionally, the obtained modeling results have revealed that the combination of relatively less active catalyst (Cu/ZSM-5/s) with the metallic structured support may considerably influence the gas exhaust cleaning process. For the great majority of applications, the combination of high surface area carriers in combination with the active catalysts strongly influences the catalytic reactions at elevated temperatures. The application of structured catalytic supports is extremely important at fast catalytic reaction, where the weak transport parameters may considerably limit the reactor yield. On the other hand, the impact of pressure drop on the technological process economy cannot be neglected. Despite the fact that monolith structure has an unarguable lowest flow resistance (Figure 3), the use of foam structure can be considered as a good alternative for monoliths in processes where the low installation dimensions are crucial.

4. Materials and Methods

As the catalyst carriers (reactor internals), stainless steel wire gauze, the nickel-chromium (NC 2733) foam (Recemat B.V., Naarden, The Netherlands) of the pore density (pores per inch—PPI) within 27 ÷ 33 (according to the producer's specification) and 100 cpsi ceramic monolith were used. The detailed support characteristics are summarised in Table 3.

Table 3. Reactor parameters used during the modelling: geometric parameters of reactor support, average Reynolds numbers, heat and mass transfer correlations (gas velocity v_m = 1 m/s).

Reactor Support	D_h, mm	a, m^{-1}	Mesh/PPI/cpsi	L, mm	Re	Heat and Mass Transfer Equation
Wire gauze [27]	0.699	4005	30.48	d_w = 0.30	25	$Nu = \frac{2\left[(4/\pi)\cdot L^{*H}\right]^{-1/2}}{\left[1+(Pr/0.0207)^{2/3}\right]^{1/4}}\left(0.270\cdot\left(Pr\cdot L^{*H}\right)^{-0.213}\right)$ $Sh = \frac{2\left[(4/\pi)\cdot L^{*M}\right]^{-1/2}}{\left[1+(Sc/0.0207)^{2/3}\right]^{1/4}}\left(0.270\cdot\left(Sc\cdot L^{*M}\right)^{-0.213}\right)$
Metal foam (NC2733) *	0.961	3615	27–33	d_s = 0.14	35	$Nu = \frac{2\left[(4/\pi)L^{*H}\right]^{-1/2}}{\left[1+(Pr/0{,}0207)^{2/3}\right]^{1/4}}\left(0,1\left(Pr\cdot L^{*H}\right)^{-0,19}\right)$ $Sh = \frac{2\left[(4/\pi)L^{*M}\right]^{-1/2}}{\left[1+(Sc/0{,}0207)^{2/3}\right]^{1/4}}\left(0,1\left(Sc\cdot L^{*M}\right)^{-0,19}\right)$
Monolith [28,29]	2.15	1399	100	L_R	80	$Nu = 3.608\left(1+\frac{0.095}{L^{*H}}\right)^{0.45}$ $Sh = 3.608\left(1+\frac{0.095}{L^{*M}}\right)^{0.45}$

* Heat transfer equation is derived based on own experiments. The methodology is the same as in [25]. Mass transfer description is derived using Chilton–Colburn analogy as confirmed by Giani et al. [30,31] PPI = pores per inch; cpsi = channels (cells) per square inch.

4.1. Catalyst Preparation and Characterization

In this study, two zeolite catalysts, MFI-type zeolite with Si/Al = 37 and ultrastabilized Y with Si/Al = 4.52, were used. The zeolites with MFI-type structure containing a different aluminum content were synthesized according to the following procedure. Gels of defined chemical composition were prepared in several steps. In the first step, aluminum nitrate nonahydrate (Chempur, p.a., Piekary Śląskie, Poland) was dissolved in aqueous solution of sodium hydroxide (Chempur, p.a.). The second solution was obtained by adding a template, i.e., tetrapropylammonium bromide (TPABr, Sigma Aldrich, 98%, Poznań, Poland), to the NaOH solution. The obtained solutions were mixed with silica (Zeosil, 98%, Gorzów Wlkp., Poland) under vigorous stirring and aged for 20 h at ambient conditions. The aged gels were subsequently placed into Teflon-lined stainless-steel autoclaves, sealed and kept at 175 °C for 20 h. The autoclaves were rotated at 56 rpm. The obtained solids were centrifuged, washed and dried at 80 °C. In order to remove organic template (TPABr) the obtained zeolites were calcined at 480 °C for 8 h with temperature ramp of 2 °C/min. Y-type zeolite was synthesized under the following conditions. In the first step, sodium aluminate (Riedel de Haën, p.a., Seelze, Germany) was dissolved in aqueous solution of sodium hydroxide (Chempur, p.a.). Subsequently, colloidal silica (Ludox AS-40, 40%) was added under vigorous stirring. The obtained gel was then placed into Teflon-lined stainless-steel autoclave, sealed and kept at room temperature for 24 h. Subsequently, the autoclave was placed in a furnace at 95 °C for the next 24 h in static conditions. After synthesis, the solids were centrifuged, washed and dried at 80 °C. In order to ultrastabilize zeolite with Y type structure, a triple ion exchange with a 0.1 M aqueous ammonium nitrate solution at 80 °C for 2 h was carried out. Subsequently, ion-exchanged samples were centrifuged and washed three times with distilled water and then dried. Obtained ammonium form of zeolite was calcined in vacuum at 700 °C for 3 h with temperature ramp of 2 °C/min in the presence of saturated water vapor under pressure 1.25 kPa. The ZSM-5 zeolite were ion-exchanged twice with a 0.1 M aqueous ammonium nitrate solution at 80 °C for 2 h. Subsequently, ion-exchanged zeolite was centrifuged and washed three times with distilled water and dried. Afterwards, samples were calcined at 450 °C for 8 h with temperature ramp of 2 °C/min and flow rate of 50 mL/min.

In the final step, the copper containing zeolite catalysts were prepared using classical ion-exchange method or sonication method. In the classical ion-exchange method, the synthesized zeolite samples were immersed in 0.5 M aqueous copper nitrate solution at 20 °C for 24 h. Subsequently, ion-exchanged samples were centrifuged and washed three times with distilled water and dried. Obtained Cu-containing zeolites were calcined in dry air at 500 °C for 4 h with temperature ramp of 2 °C/min and flow rate of 50 mL/min.

In the sonochemical method, the obtained zeolites were immersed in 0.5 M aqueous copper nitrate solutions and sonochemically irradiated for 20 min using QSonica S-4000 sonicator equipped with a $\frac{1}{2}''$ diameter horn (the average power of sonication equals 60 W and frequency 20 kHz). During the sonication procedure, the glass tube filled with the catalyst precursor was placed in ice bath to keep the temperature below 60 °C. Directly before sonication, the samples were outgassed for 15 min using Ar (Linde, 99.5%, Kraków, Poland) with flow rate of 20 mL/min, and 1.5 mL of ethanol was added to the suspension. Centrifugation, drying and calcination processes were carried out under the same conditions as above.

The catalysts were denoted as Cu/USY and Cu/ZSM-5 for catalysts prepared by using classical ion-exchange method, whereas for catalysts prepared by sonochemical method the suffix "s" was added. The catalysts preparation and characterization details are presented in Table 1.

The catalysts metal (Cu) content in the prepared catalysts samples was determined by atomic absorption spectroscopy (AAS) using Thermo Scientific ICE3000 series AAS spectrometer. The external standard method was applied for determination of metal content (AAS standards, Sigma Aldrich).

4.2. Kinetic Tests

Studies concerning selective catalytic reduction (SCR) of NO with NH_3 were performed in a fixed-bed quartz microreactor equipped with quadrupole mass spectrometer (Prevac, Rogów, Poland). The experiments were performed at atmospheric pressure and the temperature ranged from 50 to 550 °C. During the experiments, the standard mass of 0.100 g of catalyst (fractioned particles sizes in the range of 0.160–0.315 mm) was placed on quartz wool plug in the reactor. The following step consists of outgassing of the sample in a flow of pure helium at 550 °C for 1 h. Then the gas mixture containing 2500 ppm of NO, 2500 ppm of NH_3 and 25,000 ppm of O_2 balanced by helium with the total flow rate of 40 mL/min.

4.3. Reactor Modelling

4.3.1. Mass and Energy Balances

In this study, the one-dimensional (1D) plug-flow model of the reactor with structured support is considered. For this purpose, the material and energy balances are considered for both gaseous and solid phases, respectively. The material balance in the gas-phase reaction can be expressed as follows:

$$\frac{d(C_a v_m)}{dz} + ak_c(C_A - C_{AS}) = 0 \quad (1)$$

$$BC: z = 0; C_A = C_{A0}$$

The presented model ignores the homogeneous reactions. Additionally, according to the literature research, the influence of axial dispersion on the final conversion can be neglected [29,30]. Considering the reaction at the catalyst surface, it can be assumed that the mass transfer of nitrogen monoxide is balanced by chemical reaction according to the equation:

$$k_C(C_A - C_{AS}) = \eta(-R_A) = \eta k_r C_{AS} \quad (2)$$

where the term η represents the effectiveness factor of the catalyst. It can be expressed as a function of Thiele modulus ϕ [32]:

$$\eta = \frac{tgh(\phi)}{\phi}, \phi = l\sqrt{\frac{k_r}{D_{Ai}}} \quad (3)$$

where l is the catalyst layer thickness. According to our previous studies [18,19], the SEM analysis revealed that the layer thickness is ca. 20 µm for catalysts deposited on the steel support. For the catalyst beads, the catalysts layer can be calculated using formula $l = d_p/6$. The Thiele modulus as well as the effectiveness factor vary throughout the reactor and are calculated at each point of the reactor length. The average Thiele modulus and effectiveness factors for reactors modelled are summarised in Table 1.

When considering the energy balance, the temperature increase along the reactor as a result of reaction heat generation in the catalytic layer must be considered. The generated heat is subsequently transferred to the gas stream. Taking the above into account, the energy balance for the gas phase can be expressed as:

$$-v_m \rho C_p \frac{dT}{dz} + ah(T_S - T) = 0 \quad (4)$$

$$BC: z = 0; T = T_0$$

The heat produced due to the catalytic reaction is balanced by the heat transferred from the catalytic layer to the gas phase according to the equation:

$$h(T_S - T) = -\cdot H_R \eta(-R_A) \quad (5)$$

All the physical and chemical parameters (Equations (1)–(5)) were estimated for the local gas temperature. The heat losses were neglected.

4.3.2. Pressure Drop

In this study, for the modelling purposes, the performance of the structured supports was also compared in terms of pressure drop. The pressure drops were calculated using Darcy–Weisbach equation:

$$\Delta P = 2f\frac{\varrho v_{m0}^2}{\varepsilon^2 D_h}L \tag{6}$$

where, the Fanning friction factor, f, was derived experimentally for wire gauze and foam-structured supports. The detailed description of the procedure for determination of flow resistance correlations can be found in our previous studies [33,34]. The correlations describing flow resistance are summarised in Table 4.

Table 4. Flow resistance correlations.

Support	Correlation	Ref.
Wire gauze	$f = \frac{37.78}{Re} + 0.565$	[35]
Metal foam (NC2733) *	$f = \frac{53.16}{Re} + 0.53$	
Monolith	$fRe = 16\left(1 + \frac{0.0045}{L^+}\right)^{0.5}$	[29]

*—Based on own experiments, the measurement details are provided in [13,33].

4.3.3. Reaction Kinetics

According to the chemical reaction:

$$4NO + 4NH_3 + O_2 \rightarrow 4N_2 + 6H_2O \tag{7}$$

the reaction rate of SCR deNO$_x$ may be expressed as follows:

$$(-R_A) = k_r C_{NO}^a C_{NH_3}^b C_{O_2}^c C_{H_2O}^d \tag{8}$$

According to the literature data, when the ammonia, oxygen and water (vapour) are in excess, the reaction orders with respect to NH_3, O_2 and H_2O can be assumed to be zero [36]. In this study, the performance of structured reactor for catalytic SCR NO removal from biogas fuelled engines is modelled. In this case, the exhaust gases are rich with oxygen and water vapour. Additionally, the ammonia injected prior to the catalytic converter is also in excess. Finally, a first order with respect to NO was assumed, as determined in [36]. The final equation expressing the rate of the SCR deNO$_X$ reaction considered in this study can be presented in the following form:

$$(-R_A) = k_r C_A = k_\infty exp\left(\frac{-E_A}{R_g T}\right)C_A \tag{9}$$

4.3.4. Modelling Conditions

In this study, the performance of three structured reactors with the deposited catalyst are modelled:

- stacked wire gauze sheets (30.48 meshes per inch, D$_h$ = 0.699 mm) [35];
- classic multi-channel monoliths 100 cpsi (channels (cells) per square inch) [29];
- metal foam structure (NC2733) (27–33 pores per inch, D$_h$ = 0.961 mm).

Detailed information about the foam structure parameters is presented in Appendix A.
During the modelling, the following conditions were used:

- for the reaction: $4NO + 4NH_3 + O_2 \rightarrow 4N_2 + 6H_2O$ the heat of reaction at the catalyst surface was determined to be, $\Delta H^{\circ}{}_R = -407$ kJ/mol;
- properties along the channel change as a function of the local temperature;
- the inlet NO concentration equals 2500 ppm (complete conversion obtained for prepared catalysts);
- the inlet gas temperature equals 573 K;
- the gas superficial velocity equals 1 m/s; the corresponding Reynolds numbers are given in Table 2.

The performance of the three structured reactors was performed in Matlab R2011a software (the discretization level was set to 25 points). The developed first-order differential equations were solved by using Euler method. The accuracy of the developed model was previously confirmed in [35,37] for n-hexane catalytic combustion.

The heat and mass transfer characteristics for the stacked wire gauze sheets and metal foam structures were obtained experimentally by using the methodology presented in [13,35]. For the classical ceramic monolith, the literature data were used [7,29]. The heat and transfer characteristics used during the modelling are summarised in Table 1.

The heat and mass transfer characteristics for three types of the structured reactors were expressed using the nomenclature by Shah and London [31]. The dimensionless criterion Nusselt (Nu) and Sherwood (Sh) numbers, are presented as functions of the heat (or mass) dimensionless channel length L^{*H} (L^{*M}) [31]:

$$Nu = \frac{hD_h}{\lambda} = f\left(L^{*H}\right) \quad (10)$$

$$L^{*H} = \frac{L}{D_h RePr} \quad (11)$$

$$Sh = \frac{k_C D_h}{D_A} = f\left(L^{*M}\right) \quad (12)$$

$$L^{*M} = \frac{L}{D_h ReSc} \quad (13)$$

where, L is the characteristic channel length. The characteristic channel length varies, depending on the structure used, i.e., for monolith it is the reactor length, for wire gauze, L is equal to the wire diameter d_w, and for metal foam, L is equal to the strut diameter.

The hydraulic diameter, assuming that the channel cross-sectional shape can be neglected, the hydraulic diameters for wire gauze and metal foam supports can be expressed as follows:

$$D_h = 4\varepsilon/a \quad (14)$$

whereas for monolith

$$D_h = 4A/P \quad (15)$$

5. Conclusions

The aim of this study was to compare the performance of the three structured supports with deposited Cu zeolite-based catalysts in $deNO_x$ SCR reaction. The catalysts prepared via sonochemical route have revealed an extraordinary activity in SCR $deNO_x$ by achieving the maximum conversion with almost constant 100% selectivity towards the N_2. The 1D modelling of the structured catalysts have proved that the reactor carriers have a profound impact on the overall reactor performance. Over the modelled catalytic supports, the best performance represented by the length required for the 90% conversion was achieved by the reactor with stacked wire gauzes. The comparable performance was represented by metallic foams. Taking into account the pressure drop calculation results, the metallic foams can be considered as a good alternative for ceramic monoliths in $deNO_x$ removal from stationary sources.

Acknowledgments: Financial support for this work was provided by the National Centre for Research and Development LIDER/204/L-6/14/ NCBR/2015 and partly within Polish National Science Centre—Project No. 2015/17/D/ST8/01252, 2011/03/B/ST8/05455 and 2016/21/B/ST8/00496.

Author Contributions: Przemysław J. Jodłowski designed the study, developed the model presented and carried out the model from experimental data. Łukasz Kuterasiński, Roman J. Jędrzejczyk and Damian Chlebda synthetized and characterized zeolite catalysts. Anna Garncarczyk performed heat and mass transport experiments. Sylwia Basąg and Lucjan Chmielarz performed catalytic tests. All authors read and approved the manuscript prior to submission.

Conflicts of Interest: The authors declare no conflict of interest.

Appendix A

List of Symbols:

A	channel cross-sectional surface area, m^2
A	specific surface area, m^{-1}
C_A, C_{AS}	mean reactant A concentration in bulk gas phase, at catalyst external surface, respectively, mol/m^3
C_p	heat capacity, J/mol·K
dp	sphere diameter, m
D_h	hydraulic diameter, m
D_A, D_{Ai}	molecular diffusivity; internal diffusivity (in porous catalyst), respectively; m^2/s
d_s	strut diameter (foam), m
d_w	wire diameter (wire gauze), m
E_A	apparent activation energy, J/mol
f	Fanning friction factor
h	heat transfer coefficient, $W/m^2 \cdot K$
ΔH°_R	standard heat of reaction, J/mol
k_r	reaction rate constant, m/s
k_C	mass transfer coefficient, m/s
k_∞	pre-exponential coefficient in Arrhenius equation, m/s
$k_{eff\,-}$	effective reaction rate constant, m/s
L, L_R	channel or reactor length, respectively, m
L^{*H}, L^{*M}	heat or mass dimensionless channel length, respectively
L^+	dimensional channel length, $L^+ = \frac{L}{D_h Re}$
L	diffusion path length in the catalytic phase, m
M_{cat}	Mass of catalyst, kg/m^2
Nu	Nusselt number, hD_h/λ
Pr	Prandtl number, $C_p \nu \rho/\lambda$
P	channel perimeter, m
ΔP	pressure drop, Pa
$(-R_A)$	reaction rate, $mol/(m^2 \cdot s)$
Re	Reynolds number, $v_m D_h/\nu$
Sc	Schmidt number, ν/D_A
Sh	Sherwood number, $k_C D_h/D_A$
T	temperature, K
v_m	superficial gas velocity, m/s
z	reactor axis, m
ε	bed or structure void volume (external packing porosity), dimensionless
η	effectiveness factor for catalyst
λ	heat conductivity, W/mK
ϕ	Thiele modulus, Equation (3)
ν	kinematic viscosity

Subscripts

A	relating to species A
AS	relating to adsorbed species A, surface value
0	refers to reactor inlet
S	refers to catalyst surface

References

1. Chen, H.; Wei, Z.; Kollar, M.; Gao, F.; Wang, Y.; Szanyi, J.; Peden, C.H.F. A comparative study of N_2O formation during the selective catalytic reduction of NO_x with NH_3 on zeolite supported Cu catalysts. *J. Catal.* **2015**, *329*, 490–498. [CrossRef]
2. Li, S.; Chen, Z.; He, E.; Jiang, B.; Li, Z.; Wang, Q. Combustion characteristics and NO_x formation of a retrofitted low-volatile coal-fired 330 MW utility boiler under various loads with deep-air-staging. *Appl. Therm. Eng.* **2017**, *110*, 223–233. [CrossRef]
3. Roy, S.; Hegde, M.S.; Madras, G. Catalysis for NO_x abatement. *Appl. Energy* **2009**, *86*, 2283–2297. [CrossRef]
4. Carabineiro, S.A.C.; Lobo, L.S. Understanding the Reactions of CO_2, NO, and N_2O with Activated Carbon Catalyzed by Binary Mixtures. *Energy Fuels* **2016**, *30*, 6881–6891. [CrossRef]
5. Carabineiro, S.A.; Fernandes, F.B.; Vital, J.S.; Ramos, A.M.; Silva, I.F. Uncatalyzed and catalyzed NO and N2O reaction using various catalysts and binary barium mixtures supported on activated carbon. *Catal. Today* **1999**, *54*, 559–567. [CrossRef]
6. BTG Biomass Technology Group BV. *Handbook of Biomass Gasification*; Knoef, H.A.M., Ed.; BTG Biomass Technology Group BV: Enschede, The Netherlands, 2005.
7. Cybulski, A.; Moulijn, J.A. *Structured Catalysts and Reactors*; Chemical Industries; Taylor & Francis: Abingdon, UK, 2006.
8. Busca, G.; Kennedy, P.J.F. Acidity and basicity of zeolites: A fundamental approach. *Microporous Mesoporous Mater.* **2017**, 1–14. [CrossRef]
9. Vaiciukyniene, D.; Kantautas, A.; Vaitkevicius, V.; Jakevicius, L.; Rudzionis, Z.; Paskevicius, M. Effects of ultrasonic treatment on zeolite NaA synthesized from by-product silica. *Ultrason. Sonochem.* **2015**, *27*, 515–521. [CrossRef] [PubMed]
10. Wang, B.; Wu, J.; Yuan, Z.-Y.; Li, N.; Xiang, S. Synthesis of MCM-22 zeolite by an ultrasonic-assisted aging procedure. *Ultrason. Sonochem.* **2008**, *15*, 334–338. [CrossRef] [PubMed]
11. Belviso, C.; Cavalcante, F.; Lettino, A.; Fiore, S. Ultrasonics Sonochemistry Effects of ultrasonic treatment on zeolite synthesized from coal fly ash. *Ultrason. Sonochem.* **2011**, *18*, 661–668. [CrossRef] [PubMed]
12. Kryca, J.; Iwaniszyn, M.; Piątek, M.; Jodłowski, P.J.; Jędrzejczyk, R.; Pędrys, R.; Wróbel, A.; Łojewska, J.; Kołodziej, A. Structured Foam Reactor with CuSSZ-13 Catalyst for SCR of NO_x with Ammonia. *Top. Catal.* **2016**, *59*, 887–894. [CrossRef]
13. Gancarczyk, A.; Piątek, M.; Iwaniszyn, M.; Jodłowski, P.J.; Łojewska, J.; Kowalska, J.; Kołodziej, A. In Search of Governing Gas Flow Mechanism through Metal Solid Foams. *Catalysts* **2017**, *7*, 124. [CrossRef]
14. Iwaniszyn, M.; Piątek, M.; Gancarczyk, A.; Jodłowski, P.J.; Łojewska, J.; Kołodziej, A. Flow resistance and heat transfer in short channels of metallic monoliths: Experiments versus CFD. *Int. J. Heat Mass Transf.* **2017**, *109*, 778–785. [CrossRef]
15. Łojewska, J.; Knapik, A.; Jodłowski, P.; Łojewski, T.; Kołodziej, A. Topography and morphology of multicomponent catalytic materials based on Co, Ce and Pd oxides deposited on metallic structured carriers studied by AFM/Raman interlaced microscopes. *Catal. Today* **2013**, *216*, 11–17. [CrossRef]
16. Jodłowski, P.J.; Gołąb, R.; Kryca, J.; Kołodziej, A.; Iwaniszyn, M.; Kolaczkowski, S.T.; Łojewska, J. A Comparison Between Monolithic and Wire Gauze Structured Catalytic Reactors for CH4 and CO Removal from Biogas-Fuelled Engine Exhaust. *Top. Catal.* **2013**, *56*, 390–396. [CrossRef]
17. Kryca, J.; Jodłowski, P.J.; Iwaniszyn, M.; Gil, B.; Sitarz, M.; Kołodziej, A.; Łojewska, T.; Łojewska, J. Cu SSZ-13 zeolite catalyst on metallic foam support for SCR of NO_x with ammonia: Catalyst layering and characterisation of active sites. *Catal. Today* **2016**, *268*, 142–149. [CrossRef]

18. Ochońska, J.; Rogulska, A.; Jodłowski, P.J.; Iwaniszyn, M.; Michalik, M.; Łasocha, W.; Kołodziej, A.; Łojewska, J. Prospective Catalytic Structured Converters for NH_3-SCR of NO_x from Biogas Stationary Engines: In Situ Template-Free Synthesis of ZSM-5 Cu Exchanged Catalysts on Steel Carriers. *Top. Catal.* **2013**, *56*, 56–61. [CrossRef]
19. Ochońska, J.; McClymont, D.; Jodłowski, P.J.; Knapik, A.; Gil, B.; Makowski, W.; Łasocha, W.; Kołodziej, A.; Kolaczkowski, S.T.; Łojewska, J. Copper exchanged ultrastable zeolite Y—A catalyst for NH3-SCR of NOx from stationary biogas engines. *Catal. Today* **2012**, *191*, 6–11. [CrossRef]
20. Brandenberger, S.; Kröcher, O.; Tissler, A.; Althoff, R. The State of the Art in Selective Catalytic Reduction of NO_x by Ammonia Using Metal-Exchanged Zeolite Catalysts. *Catal. Rev.* **2008**, *50*, 492–531. [CrossRef]
21. Komatsu, T.; Nunokawa, M.; Moon, I.L.; Takahara, T.; Namba, S.; Yashima, T. Kinetic Studies of Reduction of Nitric Oxide with Ammonia on Cu2+-Exchanged Zeolites. *J. Catal.* **1994**, *148*, 427–437. [CrossRef]
22. Yu, C.; Huang, B.; Dong, L.; Chen, F.; Liu, X. In situ FT-IR study of highly dispersed MnO_x/SAPO-34 catalyst for low-temperature selective catalytic reduction of NOx by NH_3. *Catal. Today* **2016**, *281*, 610–620. [CrossRef]
23. Rutkowska, M.; Pacia, I.; Basąg, S.; Kowalczyk, A.; Piwowarska, Z.; Duda, M.; Tarach, K.A.; Góra-Marek, K.; Michalik, M.; Díaz, U. Catalytic performance of commercial Cu-ZSM-5 zeolite modified by desilication in NH_3-SCR and NH_3-SCO processes. *Microporous Mesoporous Mater.* **2017**, *246*, 193–206. [CrossRef]
24. Sanz, O.; Velasco, I.; Reyero, I.; Legorburu, I.; Arzamendi, G.; Gandía, L.M.; Montes, M. Effect of the thermal conductivity of metallic monoliths on methanolsteam reforming. *Catal. Today* **2016**, *273*, 131–139. [CrossRef]
25. Aghaei, P.; Visconti, C.G.; Groppi, G.; Tronconi, E. Development of a heat transport model for open-cell metal foams with high cell densities. *Chem. Eng. J.* **2017**, *321*, 432–446. [CrossRef]
26. Bianchi, E.; Heidig, T.; Visconti, C.G.; Groppi, G.; Freund, H.; Tronconi, E. Heat transfer properties of metal foam supports for structured catalysts: Wall heat transfer coefficient. *Catal. Today* **2013**, *216*, 121–134. [CrossRef]
27. Kołodziej, A.; Łojewska, J. Mass transfer for woven and knitted wire gauze substrates: Experiments and modelling. *Catal. Today* **2009**, *147S*, 120–124. [CrossRef]
28. Hayes, R.; Kolaczkowski, S.T. A study of Nusselt and Sherwood numbers in a monolith reactor. *Catal. Today* **1999**, *47*, 295–303. [CrossRef]
29. Hawthorn, R.D. Afterburner catalysts effects of heat and mass transfer between gas and catalyst surface. *AIChE Symp. Ser.* **1974**, *70*, 428.
30. Giani, L.; Groppi, G.; Tronconi, E. Heat Transfer Characterisation of Metallic Foams. *Ind. Eng. Chem. Res.* **2005**, *44*, 9078–9085. [CrossRef]
31. Shah, R.K.; London, A.L. *Laminar Flow Forced Convection in Ducts: A Source Book for Compact Heat Exchanger Analytical Data*; Academic Press: New York, NY, USA, 1978.
32. Sharratt, P.N.; Mann, R. Some observations on the variation of tortuosity with Thiele modulus and pore size distribution. *Chem. Eng. Sci.* **1987**, *42*, 1565–1576. [CrossRef]
33. Piątek, M.; Garncarczyk, A.; Iwaniszyn, M.; Jodłowski, P.J.; Łojewska, J.; Kołodziej, A. Gas-Phase Flow Resistance of Metal Foams: Experiments and Modeling. *AIChE J.* **2017**. [CrossRef]
34. Kołodziej, A.; Łojewska, J.; Jaroszyński, M.; Gancarczyk, A.; Jodłowski, P. Heat transfer and flow resistance for stacked wire gauzes: Experiments and modelling. *Int. J. Heat Fluid Flow* **2012**, *33*, 101–108. [CrossRef]
35. Kołodziej, A.; Łojewska, J. Experimental and modelling study on flow resistance of wire gauzes. *Chem. Eng. Process.* **2009**, *48*, 816–822. [CrossRef]
36. Koebel, M.; Elsner, M. Selective catalytic reduction of NO over commercial DeNOx-catalysts: Experimental determination of kinetic and thermodynamic parameters. *Chem. Eng. Sci.* **1998**, *53*, 657–669. [CrossRef]
37. Kołodziej, A.; Łojewska, J.; Tyczkowski, J.; Jodłowski, P.; Redzynia, W.; Iwaniszyn, M.; Zapotoczny, S.; Kuśtrowski, P. Coupled engineering and chemical approach to the design of a catalytic structured reactor for combustion of VOCs: Cobalt oxide catalyst on knitted wire gauzes. *Chem. Eng. J.* **2012**, *200*, 329–337. [CrossRef]